LAWRENCE
LIVERMORE
NATIONAL
LABORATORY

LLNL-JRNL-406015

Melting of Ice under Pressure

E. Schwegler, M. Sharma, F. Gygi, G. Galli

August 4, 2008

Proceedings of the National Academy of Sciences

Disclaimer

Melting of Ice under Pressure

Eric Schwegler[1,4], Manu Sharma[2], François Gygi[1,3] and Giulia Galli[1,2]
[1]Lawrence Livermore National Laboratory, 7000 East Ave., Livermore CA 94550
[2]Department of Chemistry, University of California, Davis CA 95616[3]Department of Applied Science, University of California, Davis CA 95616

[4]To whom correspondence should be addressed. E-mail: schwegler@llnl.gov

The melting of ice under pressure is investigated with a series of first principles molecular dynamics simulations. In particular, a two-phase approach is used to determine the melting temperature of the ice-VII phase in the range of 10 to 50 GPa. Our computed melting temperatures are consistent with existing diamond anvil cell experiments. We find that for pressures between 10 to 40 GPa, ice melts as a molecular solid. For pressures above ~45 GPa there is a sharp increase in the slope of the melting curve due to the presence of molecular dissociation and proton diffusion in the solid, prior to melting. The onset of significant proton diffusion in ice-VII as a function of increasing temperature is found to be gradual and bears many similarities to that of a type-II superionic solid.

Abbreviations: bcc, body-centered-cubic; FPMD, first principles molecular dynamics; MSD, mean-squared displacement; GPa, gigapascal.

The determination of the melting curve of water is important to many fields of science, including physics, chemistry and planetary science. For example, it has been suggested that the cold subduction zones in Earth are likely to intersect with the high-pressure melting curve of water, which would have profound implications for the chemical composition and transport of materials in the interior as well as the long-term evolution of the planet as it cools[1]. It is then quite surprising that as recently as four years ago, experimental measurements of the melting temperature (T_m) of ice in the range of 10 to 20 GPa have differed by up to 20%[2,3]. However, with advances in combining techniques such as angle-dispersive synchrotron X-ray diffraction or in situ optical Raman spectroscopy with improved diamond anvil cell technologies, many discrepancies between different measurements have been resolved and it is now possible to accurately measure the melting temperature of ice to within a few percent for pressures up to 20 GPa[3,4,5,6]. For pressures above 20 GPa, only few experiments are available and at ~50 GPa the most recently reported values of T_m[5,6,7] (see Fig. 1) exhibit significant differences with each other. Despite these large quantitative discrepancies, all of the experimental reports have found evidence of a sharp increase in the melting curve slope at approximately 35-45 GPa, which opens up the possibility that water exists as a solid in the deep interiors of planets such as Neptune, Uranus and Earth[5,8,9].

In addition to various experimental measurements, numerous first principles investigations of the properties of high-pressure water and ice have been carried out[6,10,11,12,13,14,15,18]. In particular, in Ref. [12] it was first predicted that for pressures near 30 GPa, the slope of the melting curve should increase rapidly due to the appearance of a

superionic solid phase. A superionic conductor is a material that exhibits an ionic conductivity greater than 1 $(\Omega\ \mathrm{cm})^{-1}$ in the solid phase[16]. In the case of water, the superionic phase was predicted to stem from molecular dissociation leading to fast proton diffusion within a stable body-centered cubic (*bcc*) sub-lattice of oxygen atoms. Subsequent first principles studies have reported a similar behavior[18]. Although these theoretical investigations are in overall agreement about the existence of a superionic phase, they are in poor agreement with each other regarding the location of the melting curve of ice as a function of pressure. In particular, different simulations have indicated that at 2000 K, ice will melt at pressures ranging from 30 GPa[12] to 65 GPa[6] or to 75 GPa[18]. These large differences are puzzling given that a nearly identical level of theory was employed. In addition to possible issues related to finite size effects and simulation timescales, these discrepancies may come from the choice of the computational approaches used to locate the solid-liquid phase boundary. Specifically, all of the previous reports were based on single-phase simulations (starting from either the solid or the liquid phase) and carried out with a "heat-until-it-melts" or a "squeeze-until-it-freezes" strategy for locating the transition between the liquid and the solid phase. The concern is that these techniques may lead to regimes where the solid is super-heated[19]. For example, superheating effects in ice can be clearly seen in a number of existing single-phase simulation studies using classical potentials[20,21], as well as in ultrafast temperature jump[22,23] and dynamic compression[24,25] experiments.

Here we report on the determination of the melting curve of ice up to 50 GPa, as obtained using a two-phase simulation method[26] and first principles molecular dynamics (FPMD) simulations. In addition, we discuss the onset of molecular dissociation under pressure, which is found to be a gradual process; our simulations indicate that hydrogen diffusion in the solid before melting bears many similarities to that of diffusing species in type-II superionic solids. For pressures above 30 GPa, our results are consistent with the diamond anvil cell experimental measurements reported in Ref. [7] as well as with the upper bound values from Ref. [5], and they are systematically higher than those reported in Ref. [6].

Before determining the melting curve of ice with the two-phase approach, we investigated the behavior of high-pressure ice as a function of temperature, by carrying out a series of large-scale FPMD simulations. This initial investigation is similar to several previous studies where a "heat-until-it-melts" approach was used, except for the larger simulation sizes adopted in the present case (128 instead of 32[12] or 54[6,18] molecules). For the pressure range of interest (10 to 90 GPa) ice-VII is the stable solid phase above 300 K. Ice-VII is a molecular solid with oxygen atoms arranged on a *bcc* lattice and disordered hydrogen atoms. The overall structure is often described as two interpenetrating hydrogen-bonded networks of cubic ice that are not connected to each other, as they do not share any hydrogen bonds.

The starting configurations for our simulations were generated by placing 128 oxygen atoms on a *bcc* lattice and, by using a Monte Carlo procedure, 256 hydrogen atoms[28] were included in a random fashion, in such a way as to minimize the net dipole moment and maintain Pauling's ice-rules[29]. Constant pressure and temperature simulations were

carried out at 30, 50, 70 and 90 GPa and at 400 K. After equilibrating the system for 5 ps, statistics were collected for 5 ps followed by repeated 400 K temperature increases in the range of 400 to 4000 K.

In Fig. 2, the change in the average lattice parameter as a function of the simulation temperature is shown for three different isobars. For temperatures below ~1200 K, the initial increase in the lattice parameter with temperature is approximately linear, and at higher temperatures an inflection point near 1500 K can clearly be seen in the 50 GPa simulations. For the higher pressure simulations, similar (although increasingly less pronounced) changes can be found at higher temperatures. Along the 50 GPa isobar, the MD run at 1400 K was carried out twice: once by heating from the sample at 1200 K and once by cooling from the sample at 1600 K. Identical average cell parameters were obtained in both cases, thus indicating that the transition occurs smoothly, with little or no hysterisis effects.

The reason for the rapid increase in cell size found in Fig. 2 can be understood by examining the mean-squared displacement (MSD) of the oxygen and hydrogen atoms in our simulations. For example, in Fig. 3a the MSD of the oxygen and hydrogen atoms collected from the simulation at 50 GPa and 1200 K is shown. After the initial ballistic region, the MSDs of both the hydrogen and oxygen atoms quickly level off, indicating that neither species was diffusive. A structural analysis of the trajectory confirmed that the original ice-VII structure was preserved throughout the simulation. In Fig. 3b, a similar MSD analysis is displayed for the simulation at 50 GPa and 1400 K. After approximately 0.5 ps, the hydrogen atoms start diffusing while the oxygen atoms oscillate around their *bcc* lattice sites (*i.e.* the system begins to behave as a superionic solid[12]). Further increases in temperature resulted in faster hydrogen diffusion within the stable *bcc* oxygen sublattice until very high simulation temperatures (not shown) were reached. For example, in the 50 GPa run the entire system became diffussive only when the temperature was increased to ~3000 K. This is more than 1000 K higher than any of the existing experimental measurements of the melting temperature at 50 GPa[5,6,7]; hence it is reasonable to assume that in these simulations the sample has been superheated past the melting temperature . If the differences with experiment observed here are indeed due to significant superheating effects, then the inflection points seen Fig. 2 may correspond to conditions attained in a solid superheated above melting.

In order to avoid possible superheating effects of single-phase simulations, we determined the melting temperature of ice-VII with the two-phase simulation technique. This computational approach is based on a direct comparison of the liquid and the solid free energies, obtained by performing simulations of liquid-solid interfaces. The initial configurations for our simulations were generated by carrying out independent single-phase solid (ice-VII) and liquid MD simulations of 128 water molecules at identical temperatures and pressures. The solid and liquid configurations were then combined into a single cell containing a total of 256 water molecules with a small gap between the solid and liquid surfaces. After equilibrating the solid and liquid layers independently with short MD runs under constant volume and temperature conditions, an MD simulation at constant temperature and pressure was carried out until the entire system became either a

liquid or a solid (*i.e.* the system completely either melted or froze). For a given pressure, many independent simulations were carried out at different temperatures in order to recursively bisect the melting temperature to within 50 to 100 K. In nearly all of the two-phase simulations where the system froze, the oxygen atoms were found to be arranged in a complete *bcc* lattice. The only exceptions were the simulations carried out at temperatures well below the equilibrium melting point, where the liquid showed a tendency to freeze into an amorphous solid structure. Snapshots of two-phase simulation samples are displayed in Fig. 4. The transition to a single-phase, which took on average 5 to 6 ps, was determined by monitoring the atomic MSD, variations in the equilibrium volume, and by visual inspection. We note that the velocity of the solid-liquid interface is strongly dependent on the difference between the simulation temperature and the actual melting temperature[31] . In the cases considered here, where we aimed at bracketing the melting temperature within 50-100K, we expect to have interface velocities much larger than those observed in analogous calculations with empirical potentials, where the difference between simulation and melting temperatures are much smaller[32].

In Fig. 5, our predicted melting temperatures at 10, 30, 43 and 50 GPa are shown along with recent experimental measurements[7]. The point at 43 GPa was obtained by recursively bisecting along the temperature axis (at 1600 K). At each melting point, we used the Clapeyron equation and single-phase liquid and solid simulations to compute the slope of the melting curve. The computed melting temperature at 10 GPa is approximately 60 K above the most reliable experimental measurements in this range[3,4,5], possibly indicating that our theoretical predictions are systematically shifted up in temperature by 7-10%. For pressures between 10 and 30 GPa ice-VII is found to melt as a molecular solid (with no observable dissociation in the solid phase). At higher pressures, a dissociation onset is observed, that takes place at temperatures below melting. Our simulations also indicate that there is an abrupt increase in T_m at approximately 45 GPa; this temperature coincides with the calculated onset of molecular dissociation in the solid. The raise in the slope of the melting curve most likely originates from a large entropic effect due to the dissociating water molecules. As pointed out previously[13,14], the onset of dissociation in the liquid takes place at much lower pressures (at ~15 GPa) than in the solid

Our simulations suggest that for pressures above approximately 40 GPa and for temperatures below the melting curve there is a region of the phase diagram where fast hydrogen diffusion takes place, in the presence of a stable oxygen sublattice; these results are consistent with previous simulation data. However, there are significant discrepancies between our results and those present in the literature, regarding the location of the melting curve. In particular, the heat-until-it-melts approach used in Ref. [12] resulted in melting temperatures significantly higher than those obtained here. In contrast, when a squeeze-until-it-freezes approach has been used, the corresponding melting points are found at higher pressures than in our calculations. For example, at a temperature of 2000 K we find a melting pressure of approximately 50 GPa as compared to 65 GPa in Ref. [6] and 75 GPa in Ref. [18]. This discrepancy is not surprising given that high-pressure dynamic compression experiments indicate that rapidly compressing liquid water across the melting line easily results in a metastable liquid requiring 10-100 nanoseconds to

freeze[24,25]. It is also interesting to note that the onset of dissociation in the solid phase reported in Ref. [12] is nearly identical to that found here with much larger simulation cells (128 versus 32 water molecules). This insensitivity to the size of the cell is likely due to the fact that dissociation occurs gradually in the solid and does not involve a 1st order phase transition; the description of the latter would be much more sensitive to size effects or the specific computational approach.

In order to further characterize the high-pressure solid region where fast proton diffusion occurs, we have used a set of single-phase simulations to compute the proton diffusion coefficient as a function of temperature along a 50 GPa isobar. As shown in Fig. 6, at low temperatures, within 1300 to 1600 K, proton diffusion increases rapidly with temperature. This temperature interval corresponds directly to the inflection point present in Fig. 2. Visual inspection of the simulation trajectories clearly shows that in this temperature range diffusion occurs by protons hopping between neighboring oxygen sites, in a highly correlated fashion. For T > 1600 K, the protons still diffuse via hopping between neighboring oxygen sites, but the rate of change of the diffusion coefficient as a function of temperature is smaller and there is no noticeable correlations between individual dissociation events.

It is interesting to note that the overall behavior found here for hydrogen and oxygen diffusion in water at 50 GPa is similar to that of ionic species composing superionic solids, such as PbF_2. Lead fluoride is a type-II superionic solid and in such solids the onset of the superionic phase occurs gradually, and is not accompanied by a 1st order structural phase transition[16]. In type-II superionic conductors the ionic conductivity increases rapidly with T, followed by a slower increase as the melting temperature is approached, in a manner that is very similar to the temperature dependence of the proton diffusion coefficients found in our calculations (see Fig. 6). We also note that the change in the PbF_2 lattice parameter as a function of temperature is remarkably similar to the trends shown in Fig. 2[35]. This is in contrast to the well-known behavior found in type-I superionic solids, such as AgI[16], where the transition to a superionic phase occurs abruptly as the iodine sublattice undergoes a 1st order structural transition (under ambient pressure conditions) from a hexagonal wurtzite to a bcc ordering, and the Ag cations begin to diffuse rapidly.

At even lower temperatures, the dynamical properties of ice-VII have been extensively examined by theory[36,37] and experiment[6,38]. In particular, along a 300 K isotherm FPMD simulations indicate that at pressures greater than ~55 GPa, the protons in ice-VII begin to hop back and forth between neighboring oxygen atoms along hydrogen bonds. This process, which is referred to by some as a transition to "dynamical translational proton disordered" ice-VII has been investigated also at higher temperatures by monitoring the broadening of the ice-VII phonon modes in Raman spectroscopy experiments[6] and appears to have a negative slope (see Fig. 5). Although the protons become mobile as they hop between neighboring oxygen atoms, this dynamical process does not lead to significant proton diffusion (see, for example, Fig. 2d in Ref. [37] and Fig. 3 in Ref. [38]).

There are a number of different experimental measurements that could be used to directly verify the physical properties of water under pressure predicted by our simulations. In particular, measurements of protonic diffusion in high-pressure ice-VII have been carried out by monitoring the time-dependent infrared reflectance spectra of H_2O/D_2O bilayers in a diamond anvil cell[38]. Unfortunately, these experimental measurements have only been carried out along a 400 K isotherm and a simple diffusion model was used to extrapolate the data to higher temperatures; this model did not support the existence of a superionic region in the water phase diagram. It would be interesting to carry out similar measurements at higher temperatures thus avoiding the use of extrapolations. Alternatively, with recent advancements in diamond synthesis it should now be feasible to directly measure the conductivity of ice-VII at high pressures and temperatures. For instance, lithography techniques have been used to deposit tungsten electrodes directly on a diamond culit followed by additional epitaxial diamond growth[39]. In principle, these so-called "designer diamond anvil cells" could be used to measure the ionic conductivity of ice-VII as a function of temperature, which would represent the most direct probe of the proposed superionic phase in high pressure ice.

In summary, we have used FPMD simulations to investigate the melting of ice in the pressure range of 10 to 50 GPa. For pressures ranging from 10 to 30 GPa we find that ice melts as a molecular solid while for pressures above ~40 GPa, significant molecular dissociation occurs in the solid phase before melting. This onset of dissociation appears to occur gradually as ice-VII is heated and leads to a region in the phase diagram where fast proton transport occurs within a *bcc* lattice of non-diffusive oxygen atoms. The transport of protons occurs in a highly correlated fashion well below melting, and as the temperature is increased close to the melting temperature, proton diffusion becomes uncorrelated and should lead to significant ionic conductivity while in the solid phase. The overall behavior of water in this pressure range bears many similarities to a type-II superionic solid, such as PbF_2.

In order to accurately determine the melting temperature of water, we employed a two-phase simulation method that is designed to avoid the large super-heating and cooling effects that are often present in single-phase heat-until-it-melts or squeeze-until-it-freezes approaches. Our computed melting temperatures are in good quantitative agreement with recent laser-heated diamond anvil cell measurements[5,7] and confirm that for pressures close to 43 GPa, there is a significant increase in the slope of the melting curve. As pointed out previously, such a steep increase in the melting curve of water has potential implications for planetary science, and opens up the possibility that there is solid ice in the deep interiors of planets, such as Neptune, Uranus and Earth[5]. In addition, the presence of highly mobile protons with significant ionic conductivity should significantly influence the chemical, electronic and transport properties of the planets as well[41].

Methods

The FPMD simulations were based on density functional theory (DFT) and were carried out within the Qbox code[42] with Born-Oppenheimer molecular dynamics under constant pressure and temperature conditions. A time step of 10 atomic units, normconserving pseudopotentials, the Perdew-Burke-Ernzerhof generalized gradient approximation[43]

(GGA), and a plane wave basis truncated at a maximum kinetic energy cutoff of 85 Rydberg were used for all simulations. Simulations at the DFT/GGA level of theory are known to lead to significant overstructure and slow diffusion of liquid water under ambient temperature and pressure conditions as compared to experiment[44]. However most of the disagreement with experiment appears to be due to the neglect of nuclear quantum effects[45,46], and nuclear quantum effects are unlikely to have a significant influence on the high temperature properties of water of interest here.

Acknowledgments
This work was partly performed under the auspices of the U.S. Department of Energy by Lawrence Livermore National Laboratory under Contract DE-AC52-07NA27344 and partly supported by the Office of Science, U.S. Department of Energy, SciDAC grant DE-FC02-06ER46262. Use of computer resources from Lawrence Livermore National Laboratory and the Innovative and Novel Computational Impact on Theory and Experiment (INCITE) program is gratefully acknowledged.

Figures

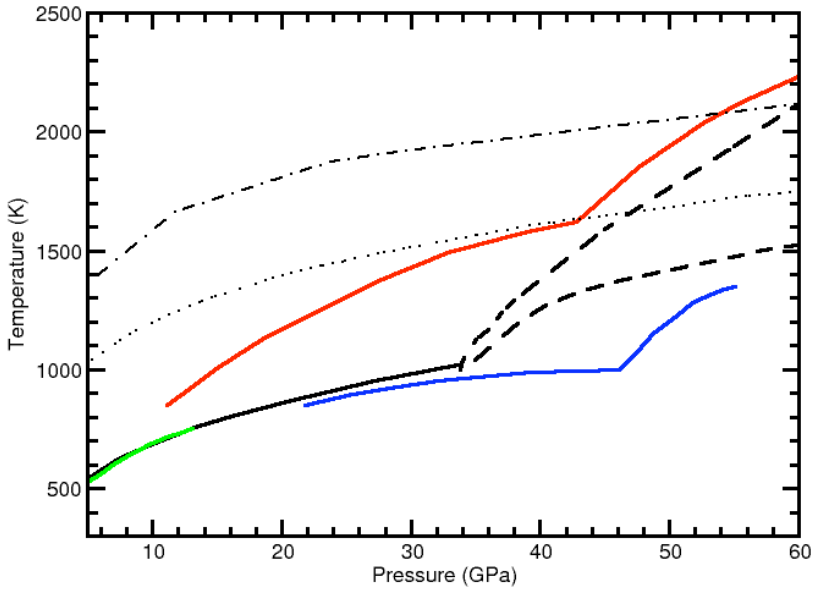

Fig. 1. Recent experimental measurements of the ice-VII melting curve as a function of pressure: Datchi, *et al.*[3] green curve, Lin, *et al.*[4] black solid curve, Schwager, *et al.*[7] red curve, and Goncharov, *et al.*[6] blue curve. The black dashed curve corresponds to the upper and lower bound of the extrapolated meting curve reported by Lin, *et al.*[5]. The Earth's geotherm[9] and the isentropes of Neptune and Uranus[8] are shown as black dashed-dotted and dotted lines, respectively.

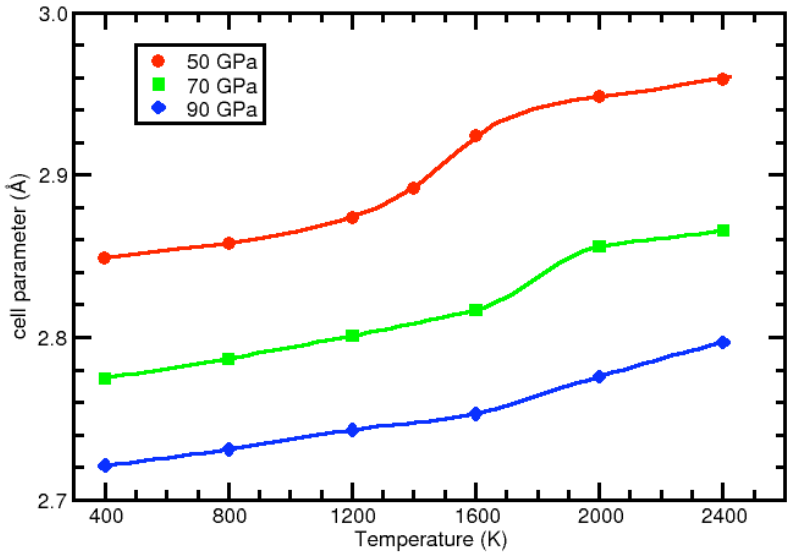

Fig. 2. The change in the average lattice parameter as a function of temperature obtained in FPMD simulations of ice-VII at 50 (red points), 70 (green points) and 90 GPa (blue points). The lines are simply a guide to the eye.

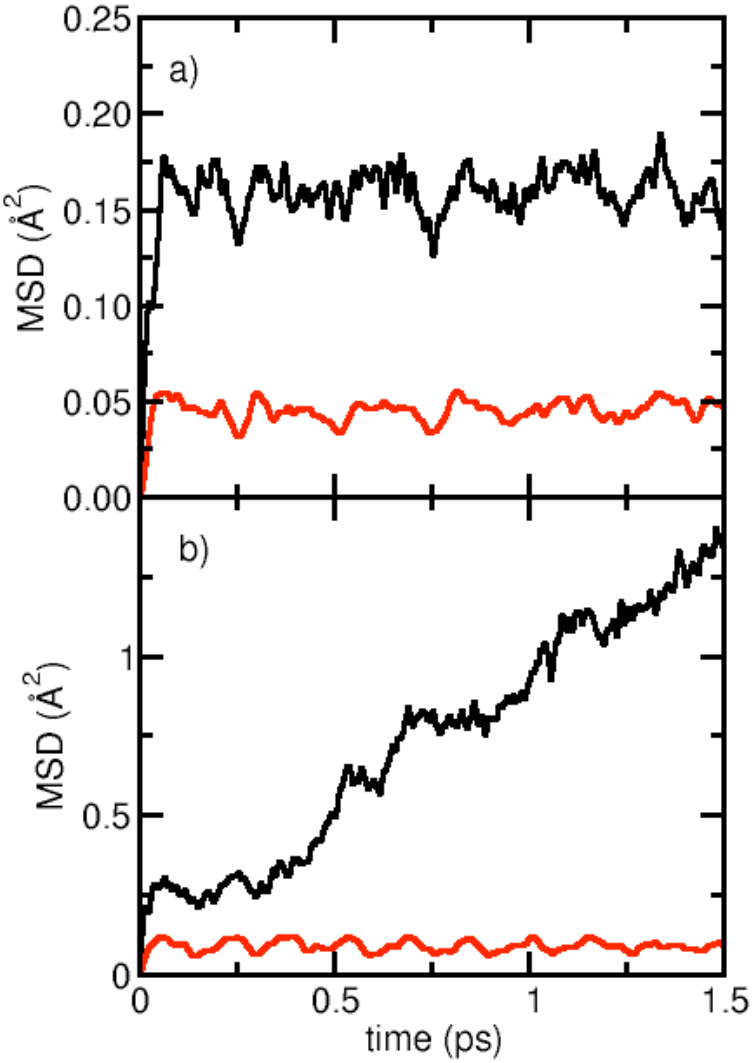

Fig. 3. The mean squared displacement of hydrogen (black curve) and oxygen (red curve) atoms in FPMD of ice-VII at a pressure of 50 GPa and a temperature of a) 1200 K and b) 1400 K.

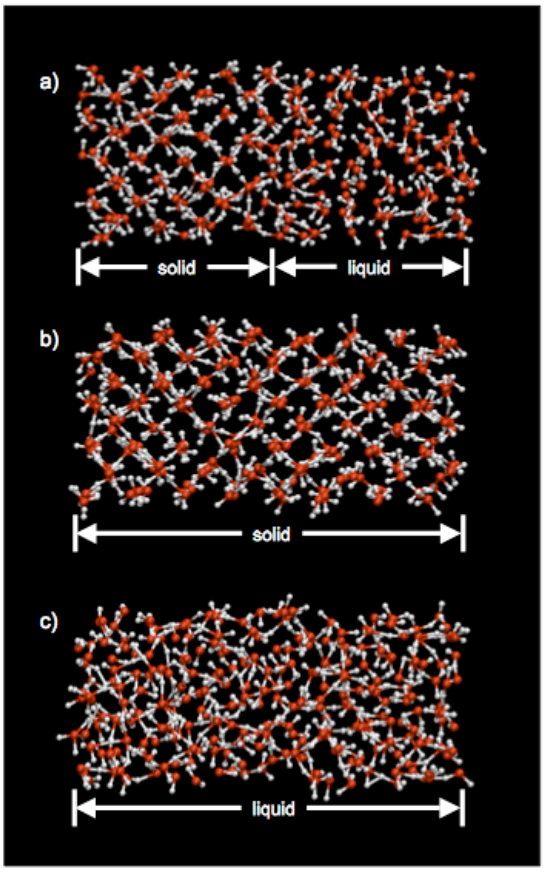

Fig. 4. Representative snapshots of two-phase simulations of water at a pressure of 50 GPa. The coordinates correspond to the initial starting configuration at 2000 K (a), to the final configuration at 2000 K (b), and to the final configuration at 2250 K (c), respectively.

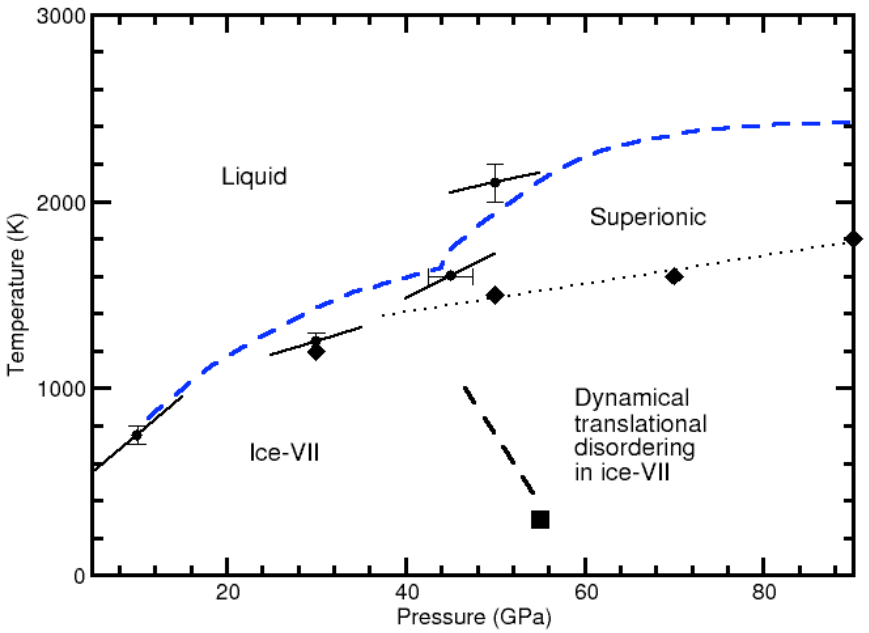

Fig. 5. The melting curve of ice at high pressure. The black circles indicate the prediction of the melting temperature from the two-phase simulation reported in this work, and the dashed diamonds correspond to the onset of significant proton diffusion in the single-phase simulations. The short black line segments centered on the computed melting points represents slopes obtained from single-phase simulations and the Clapeyron equation The blue dashed curve is the melting curve determined from the laser-heated diamond anvil cell experiments[7]. The filled black square indicates the onset of dynamical translation proton disorder in FPMD simulations of ice-VII[37], and the black dashed curve indicates the same transition in ice-VII, as identified in Raman experiments by the detection of significant broadening in the phonon mode[6].

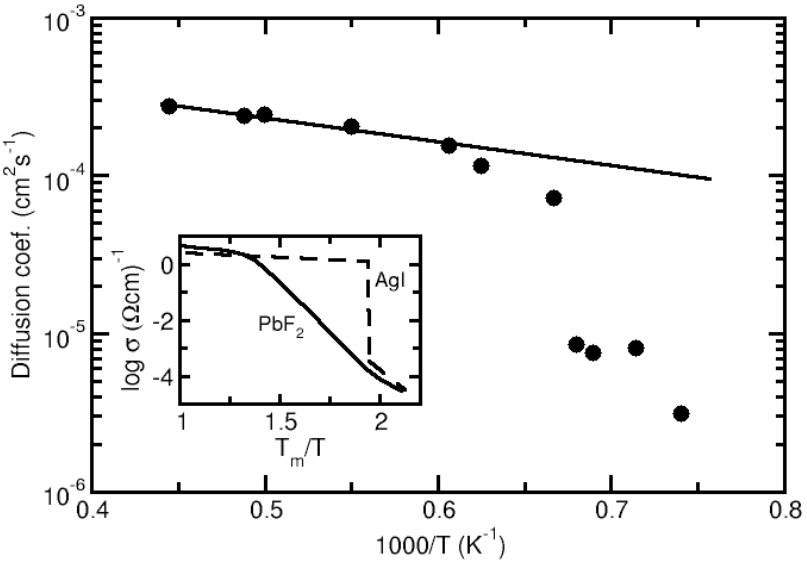

Fig. 6. The diffusion coefficient of water as a function of temperature at a pressure of 50 GPa. The inset plot shows the change in conductivity of AgI (dashed curve) and PbF_2 (solid curve), which are known type-I and type-II superionic solids, respectively (taken from Ref. [16]).

References

[1] Bina, C. R & Navrotsky, A. (2000) Possible presence of high-pressure ice in cold subducting slabs, *Nature* **408**, 844-847.

[2] Frank, M. R., Fei, Y. & Hu, J. (2004) Constraining the equation of state of fluid H_2O to 80 GPa using the melting curve, bulk modulus and thermal expansivity of Ice VII, *Geochim. Cosmochim. Acta* **68**, 2781-2790.

[3] Datchi, F., Loubeyre, P. & LeToullec, R. (2000) Extended and accurate determination of the melting curves of argon, helium, ice (H_2O), and hydrogen (H_2), *Phys. Rev. B* **61**, 6535-6546.

[4] Lin, J. F., Militzer, B., Struzkin, V. V., Gregoryanz, E. & Hemley, R. J. (2004) High pressure-temperature Raman measurements of H2O melting to 22 GPa and 900 K, *J. Chem. Phys.* **121**, 8423-8427.

[5] Lin, J. F., Gregoryanz, E., Struzhkin, V. V., Somayazulu, M., Mao, H. K. & Hemley, R. J. (2005) Melting behavior of H_2O at high pressures and temperatures, *Geophys. Res. Lett.* **32**, L11306.

[6] Goncharov, A. F., Goldman, N., Fried, L. E., Crowhurst, J. C., Kuo, I. W., Mundy, C. J. & Zaug, J. M. (2005) Dynamic Ionization of Water under Extreme Conditions*, Phys. Rev. Lett.* **94**, 125508-4.

[7] Schwager, B., Chudinovskikh, L., Gavriliuk, A. & Boehler, R. (2004) Melting curve of H_2O to 90 GPa measured in a laser-heated diamond cell, *J. Phys.: Condens. Matter* **16**, S1177-S1179.

[8] De Pater, I. & Lissauer, J. J. (2001), *Planetary Sciences*, Cambridge University Press, New York.

[9] Brown, J. M. & Shankland, T. J. (1981) Thermodynamic parameters in the Earth as determined from seismic profiles, *Geophys. J. R. Astron. Soc.* **66**, 579-596.

[10] Demontis, P., LeStar, R. & Klein, M. L. (1988) New High-Pressure Phases of Ice, *Phys. Rev. Lett.* **60**, 2284-2287.

[11] Benoit, M., Bernasconi, M., Focher, P. & Parrinello, M. (1996) New High-Pressure Phase of Ice, *Phys. Rev. Lett.* **76**, 2934-2936.

[12] Cavazzoni, C., Chiarotti, G. L., Scandolo, S., Tosatti, E., Bernasconi, M. & Parrinello, M. (1999) Superionic and Metallic States of Water and Ammonia at Giant Planet Conditions, *Science* **283**, 44-46.

[13] Schwegler, E., Galli, G. & Gygi, F. (2000) Water under Pressure, *Phys. Rev. Lett.* **84**, 2429-2432.

[14] Schwegler, E., Galli, G., Gygi, F. & Hood, R. Q. (2001) Dissociation of Water under Pressure, *Phys. Rev. Lett.* **87**, 265501-4.

[15] Mattsson, T. R. & Desjarlais, M. P. (2006) Phase diagram and electrical conductivity of high-energy-density water from density functional theory, *Phys. Rev. Lett.* **97**, 017801.

[16] Boyce, J. B. & Huberman, B. A. (1979) Superionic conductors: Transitions, structures, dynamics, *Phys. Rep.* **51**, 189-265.

[18] Goldman, N., Fried, L. E., Kuo, I. W. & Mundy, C. J. (2005) Bonding in the Supercritical Phase of Water*, Phys. Rev. Lett.* **94**, 217801-4.

[19] Belonoshko, A. B. (2001) Molecular dynamics simulations of phase transitions and melting in $MgSiO_3$ with the perovskite structure – Comment, *Amer. Miner.* **86**, 193-194.

[20] McBride, C., Vega, C., Sanz, E., MacDowell, L. G. & Abascal, J. L. F. (2005) The range of meta stability of ice-water melting for two simple models of water, *Mol. Phys*. **103**, 1-5.

[21] Luo, S. N., Strachan, A. & Swift, D. C. (2005) Deducing solid-liquid interfacial energy from superheating or supercooling: Application to H_2O at high pressure, *Model. Simul. Mater. Sci. Eng.* **13**, 321-328.

[22] Iglev, H., Schmeisser, M., Simeonidis, K., Thaller, A. & Laubereau, A. (2006) Ultrafast superheating and melting of bulk ice, *Nature* **439**, 183-186.

[23] Schmeisser, M., Iglev, H. & Laubereau, A. (2007) Bulk melting of ice at the limit of superheating, *J. Phys. Chem. B* **111**, 11271-11275.

[24] Dolan, D. H., Johnson, J. N. & Gupta, Y. M. (2005) Nanosecond freezing of water under multiple shock wave compression: Continuum modeling and wave profile measurements, *J. Chem. Phys.* **123**, 064702-10.

[25] Bastea, M., Bastea, S., Reaugh, J. E. & Reisman, D. B. (2007) Freezing kinetics in overcompressed water, *Phys. Rev. B* **75**, 172104-4.

[26] Morris, J. R., Wang, C. Z., Ho, K. M. & Chan, C. T. (1994) Melting line of aluminum from simulations of coexisting phases, *Phys. Rev. B* **49**, 3109-3115.

[28] The deuterium mass was used in all simulations to represent hydrogen.

[29] Pauling, L. (1935) The Structure and Entropy of Ice and of Other Crystals with Some Randomness of Atomic Arrangement, *J. Am. Chem. Soc.* **57**, 2680-2684.

[31] Kluge, M. D. & Ray, J. R (1989) Velocity versus temperature relation for solidification and melting of silicon: A molecular dynamics study, *Phys. Rev. B* **39**, 1738-1746.

[32] Abascal, J. L. F., Fernandez, R. G., Vega, C. & Carignano, M. A. (2006) The melting temperature of the six site potential model of water, *J. Chem. Phys*. **125**, 166101.

[35] Goff, J. P., Hayes, W., Hull, S. & Hutchings, M. T. (1991) Neutron powder diffraction study of the fast-iob transition and specific heat anomaly in β-lead fluoride, *J. Phys.: Condens. Matter* **3**, 3677-3687.

[36] Benoit, M., Marx, D. & Parrinello, M. (1998) Tunnelling and zero-point motion in high-pressure ice, *Nature* **392**, 258-261.

[37] Benoit, M., Romero, A. H. & Marx, D. (2002) Reassigning hydrogen-bond centering in dense ice, *Phys. Rev. Lett*. **89**, 145501.

[38] Katoh, E., Yamawaki, H., Fujihisa, H., Sakashita, M. & Aoki, K. (2002) Protonic Diffusion in High-Pressure Ice VII, *Science* **295**, 1264-1266.

[39] Weir, S. T., Akella, J., Vohra, Y. K. & Catledge, S. A. (2000) Epitaxial diamond encapsulation of metal microprobes for high pressure experiments, *App. Phys. Lett.* **77**, 3400-3402.

[41] Lin, J. F., Schwegler, E. & Yoo, C. S. (2006) Phase Diagram and Physical Properties of H_2O at High Pressure and Temperatures: Applications to Planetary Interiors, Earth's Deep Water Cycle, Geophysical Monograph Series **168**, 159-169.

[42] F. Gygi, *Qbox: A first-principles molecular dynamics simulation program*, Lawrence Livermore National Laboratory, 2005.

[43] Perdew, J. P., Burke, K. & Ernzerhof, M. (1996) Generalized Gradient Approximation Made Simple, *Phys. Rev. Lett.* **77**, 3865-3868.

[44] Grossman, J. C., Schwegler, E., Draeger, E. W., Gygi, F. & Galli, G. (2004) Towards an assessment of the accuracy of density functional theory for first principles simulations of water, *J. Chem. Phys.* **120**, 300.

[45] Schwegler, E., Grossman, J. C., Gygi, F. & Galli, G. (2004) Towards an assessment of the accuracy of density functional theory for first principles simulations of water II, *J. Chem. Phys.* **121**, 5400.

[46] Morrone, J. A. & Car, R. (2008) Nuclear quantum effects in water, *Phys. Rev. Lett.* **101**, 017801-4.